

the spectrum consisted of a doublet and a singlet shifted slightly upfield from the doublet center (see Figure 1).

The doublet separation was the same in each case, ruling out, for this system at least, an explanation based on diamagnetic susceptibility. The method, of course, is equally applicable to other systems.

References and Notes

- (1) H. J. C. Berendsen, *J. Chem. Phys.*, **36**, 3297-3305 (1962).
- (2) C. Migchelsen and H. J. C. Berendsen, *J. Chem. Phys.*, **59**, 296-305 (1973).
- (3) R. E. Dehl, *J. Chem. Phys.*, **48**, 831-835 (1968).

- (4) B. M. Fung, *Science*, **190**, 800 and 801 (1975).
- (5) P. Ducros, *Bull. Soc. F. Mineral. Cristallogr.*, **83**, 85-112 (1960).
- (6) J. Hougardy, W. E. E. Stone, and J. J. Fripiat, *J. Chem. Phys.*, **64**, 3840-3851 (1976).
- (7) M. P. Klein, and D. E. Phelps, *Nature (London)*, **224**, 70 and 71 (1967).
- (8) G. Chapman and K. A. McLauchlan, *Nature (London)*, **215**, 391 and 392 (1969).
- (9) G. E. Pake, *J. Chem. Phys.*, **16**, 327-336 (1948).
- (10) H. S. Gutowsky and G. E. Pake, *J. Chem. Phys.*, **18**, 162-170 (1950).
- (11) M. Shporer, A. J. Vega, and J. A. Frommer, *J. Polym. Sci.*, **12**, 645-653 (1974).
- (12) A. Abragam, "The Principles of Nuclear Magnetism", Oxford University Press, London, 1967.

Communications to the Editor

Exactly Soluble Model for High-Frequency Viscoelastic Behavior of Polymer Solutions

Experimental data^{1,2} for the high-frequency viscoelastic behavior of polymer solutions display a departure from predicted Rouse-Zimm behavior with a plateau region, $[\eta]_\infty$, in the viscosity occurring around 10^5 - 10^6 Hz for solvents with viscosities $\eta_0 \sim 10^1$ - 10^2 P. The observed $[\eta]_\infty$ is independent of molecular weight for long enough chains (e.g., polystyrene and $M \geq 2 \times 10^4$). Values of $[\eta]_\infty$ are roughly 1-2 orders of magnitude smaller than the zero-frequency values $[\eta]$ (depending on M), and $[\eta]_\infty$ is correlated to the degree of side-chain flexibility. The experimental data were originally fit¹ to the phenomenological Cerf-Peterlin theory³ of internal viscosity with a particular choice of its mode dependence, but recent calculations² with exact Rouse-Zimm eigenvalues do not reproduce the observed results. It will be of interest to determine a phenomenological form for the internal viscosity (with different mode dependence and, perhaps, frequency dependence⁴) which can satisfactorily explain the data.

Theoretical calculations of $[\eta]_\infty$ with models involving fixed bond lengths and possibly fixed bond angles give values 1.5 orders of magnitude too small,⁴⁻⁶ so these constraints cannot be responsible for the $[\eta]_\infty$. Recent Monte-Carlo calculations by Fixman⁷ for Rouse chains with fixed bond lengths and angles as well as with hindered bond rotations demonstrate that the latter feature can produce an $[\eta]_\infty$ of the correct qualitative form.

In an attempt to further understand the molecular origins of this perplexing $[\eta]_\infty$, we have introduced an exactly solvable model of polymer chain dynamics with the following important features: Side group motions are explicitly incorporated through the use of additional Rouse units. Hindered rotational potentials are simulated by side group-side group interactions. Constraints on bond lengths and angles are ignored consistent with their minor influence on $[\eta]_\infty$. Our model is one of a Rouse chain of units of type B with Kuhn length σ_B . Attached to each B unit is an A unit representing the side group, and the A-B Kuhn length is σ_A . The model differs from K stner's model⁸ of a Rouse comblike chain by having an interaction between successive A-B bond vectors, $\mathbf{y}_i - \mathbf{x}_i$, which is proportional to $(\mathbf{y}_i - \mathbf{x}_i) \cdot (\mathbf{y}_{i+1} - \mathbf{x}_{i+1})$, thereby providing hindered rotation potentials. The model is represented in Figure 1. In the absence of the hindering rotation

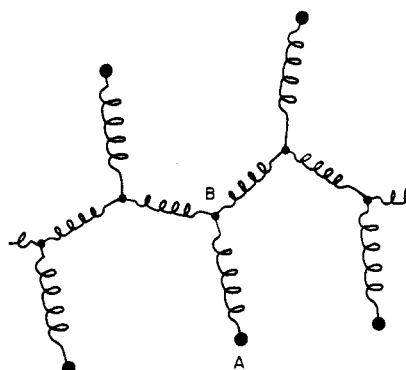


Figure 1. Schematic representation of the model. The B units correspond to an ordinary Rouse chain, while the A units (side groups) convert the chain into a comblike polymer. Interactions between neighboring AB bonds lead to hindered rotational potentials.

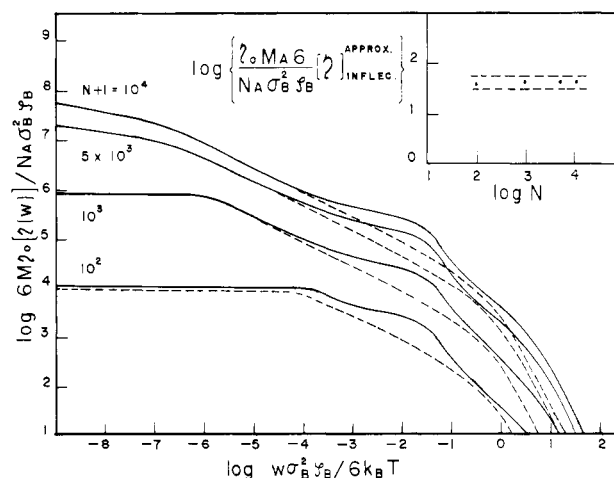


Figure 2. Plot of $\log [\eta(\omega)]$ vs. $\log \omega$ for the model (solid lines) and for a pure Rouse chain (dashed lines) where single units C_i replace a pair of A-B units. The parameters are $\gamma = 0.22$, $\epsilon_2 = 2\epsilon_3$, $\epsilon_3 = 0.125$. The curves are given for various chain lengths (N), and the insert shows that the $[\eta]_\infty$ is roughly independent of N . The dashed lines indicate approximate uncertainty in choice of $[\eta]_{\text{infection}}^{\text{approx}}$.

interaction, the A units would move in three dimensions, harmonically bound about its B unit, but the interaction tends to align the A-B bonds in syndiotactic configurations. The model can be generalized to include a preferred

ABB bond angle by the introduction of additional AB–BB bond interactions.⁹

We have determined analytical expressions for the relaxation frequencies for the model in the nondraining limit.⁹ The model displays two (\pm) branches like those discussed by Fixman and Evans;¹⁰ however, the gap between the branches is not associated with $[\eta]_\infty$. This gap is, perhaps, related to a second plateau¹¹ at higher frequencies (up by 10^2 Hz) with a calculated $[\eta]_\infty'$ down from $[\eta]$ by 10^{-2} – 10^{-5} depending on the model parameters. Neglecting terms of order N^{-1} ($N + 1$ is the number of B segments), the dimensionless relaxation frequencies, $\lambda_{k\pm}$, are given by⁹

$$\lambda_{k\pm} = \frac{1}{2}\{\lambda_k^*[1 - \frac{1}{2}\epsilon_3(1 + \gamma)] + (1 + \gamma)(\epsilon_2 + \epsilon_3)\} \pm \frac{1}{2}\{(\lambda_k^*[1 - \frac{1}{2}\epsilon_3(1 + \gamma)] + (1 + \gamma)(\epsilon_2 + \epsilon_3))^2 - 4\gamma\lambda_k^*(-\frac{1}{2}\epsilon_3\lambda_k^* + \epsilon_2 + \epsilon_3)\}^{1/2} \quad (1)$$

where $\lambda_k^* = 4 \sin^2 [\pi k/2(N + 1)]$, $\gamma = \zeta_B/\zeta_A$ is the ratio of B to A friction coefficients, $\epsilon_2 = (\sigma_B/\sigma_A)^2$, and $3k_B T \epsilon_3/2\sigma_B^2$ is the strength of the AB–AB interaction. The complex frequency dependent viscosity, $[\eta(\omega)]$, is then obtained from the familiar equation,

$$[\eta(\omega)] = \frac{N_A k_B T}{M \eta_0} \sum_{k, \alpha = \pm} \left[i\omega + \frac{6k_B T \lambda_{k\alpha}}{\sigma_B^2 \zeta_B} \right]^{-1} \quad (2)$$

We have evaluated (1) and (2) for some values of the model parameters. A slight plateau is found in the appropriate first plateau frequency regime for large side groups ($\zeta_A > \zeta_B$ and $\sigma_A > \sigma_B$), giving $[\eta]_\infty/[\eta]$ values of a reasonable order of magnitude. An example is displayed in Figure 2 (solid lines) for various values of N with the effective Rouse predictions (dashed lines) wherein the A_i-B_i units are combined into effective, C_i , Rouse ones. Note that the difference between the model and effective Rouse curves for $\omega \rightarrow 0$ and $N = 99$ arises from the $O(N^{-1})$ corrections to (1) which have been included in the calculations.⁹ Approximate values of $[\eta]_\infty$ are taken from the curves of Figure 2 from the inflection region on the curves. A plot of $[\eta]_{\text{inflection}}^{\text{approx}}$ vs. N in the insert in Figure 2 demonstrates the approximate molecular weight independence of $[\eta]_{\text{inflection}}^{\text{approx}}$ for large molecular weights in conformity with experimental $[\eta]_\infty$. (At lower molecular weights an N dependence emerges in both cases.) The plateau region in Figure 2 is not as flat and wide as observed experimentally, but perhaps this can be remedied by adjusting the parameters and by introducing additional bond angle constraints as noted above. An additional generalization involves the inclusion of non-nearest-neighbor ($i-i \pm 2$, etc.) interactions as in the model of Simon¹² which does not contain the important side-group motions.

The model is, thus, seen to display the correct qualitative form of $[\eta]_\infty$ as arising from hindered rotation potentials in agreement with the Monte-Carlo calculations of Fixman.⁷ Our model, however, explicitly includes the side groups, so studies of perpendicular dielectric relaxation¹³ and side-group contributions to flow birefringence can be made within our model.

Acknowledgment. We are grateful to Professor S. Adelman for helpful discussions and to Professor M. Fixman for sending us his papers prior to publication. This research is supported in part by NSF Grant DMR 76-82935 (polymer program) and a Camille and Henry Dreyfus Teacher–Scholar Grant to KFF.

References and Notes

- (1) J. W. M. Noordermeer, O. Kramer, F. H. M. Nestler, J. L. Schrag, and J. D. Ferry, *Macromolecules*, **8**, 539 (1975); J. W.

- M. Noordermeer, J. D. Ferry, and N. Nemoto, *ibid.*, **8**, 672 (1975).
- (2) B. G. Brueggman, M. G. Minnick, and J. L. Schrag, *Macromolecules*, **11**, 119 (1978).
- (3) A. Peterlin, *J. Polym. Sci., Part A-2*, **5**, 179 (1967); *J. Polym. Sci., Part B*, **10**, 101 (1972).
- (4) S. A. Adelman and K. F. Freed, *J. Chem. Phys.*, **67**, 1380 (1977).
- (5) M. Fixman and J. Kovac, *J. Chem. Phys.*, **61**, 4939, 4950 (1974); **63**, 935 (1975); M. Fixman and G. T. Evans, *ibid.*, **64**, 3474 (1976).
- (6) M. Doi, H. Nakajima, and Y. Wada, *Colloid Polym. Sci.*, **253**, 905 (1975); **254**, 559 (1976).
- (7) M. Fixman, *J. Chem. Phys.*, **68**, 2983 (1978).
- (8) S. Kästner, *Kolloid-Z.*, **184**, 109 (1962).
- (9) R. S. Adler and K. F. Freed, to be published.
- (10) M. Fixman and G. T. Evans, *J. Chem. Phys.*, **68**, 195 (1978).
- (11) K. Osaki and J. L. Schrag, *Polym. J.*, **2**, 541 (1971).
- (12) E. Simon, *J. Chem. Phys.*, **52**, 3879 (1970).
- (13) W. H. Stockmayer, A. A. Jones, and T. L. Treadwell, *Macromolecules*, **10**, 762 (1977).

Ronald S. Adler* and Karl F. Freed

The James Franck Institute and
The Department of Chemistry
The University of Chicago
Chicago, Illinois 60637

Received May 26, 1978

Dependence of the Electric Field-Induced Orientation of Poly(riboadenylic acid) on Its Polyelectrolyte Properties

The interpretation of the results of electrooptic measurements on the natural nucleic acids and polynucleotides has been hampered by the lack of a suitable theoretical treatment of the mechanism for the orientation of polyelectrolytes in moderate and strong electric fields. Although at least three such treatments have been attempted^{1–3} and the subject has been discussed at some length,⁴ recent advances in polyelectrolyte theory have not yet been applied successfully to this problem. In an extensive paper on the dichroism of poly(A)⁵ we demonstrated the applicability of one of the predictions of polyelectrolyte theory to electrooptic measurements, the independence or stability of the “condensed” counterion density of polyelectrolytes of sufficiently high linear charge density. In a further attempt to understand the orientation of these macromolecules in electric field, we have perturbed their ionic environment to produce predictable changes (from the recent polyelectrolyte theories of Manning,⁶ Record,⁷ Mandel,^{8,9} and McTague and Gibbs¹⁰ and their respective colleagues) in the “condensed” counterion density and observed the resulting effect on the electric-field-induced dichroism. We report here briefly one such experiment, which together with our earlier result⁵ and with other measurements¹¹ support the contention^{1,2,12} that the polarization of condensed counterions on these highly charged polyelectrolytes, as described by the polyelectrolyte theories, plays as important a role in their field-induced orientation as they do in their dielectric properties.¹³ Hogan et al.¹⁴ have recently adopted a mechanism for the electric-field-induced orientation which differs from the one advanced here and depends on the anisotropic local fields established in the vicinity of the polyelectrolyte as a result of counterion flow. The constancy of the orientation of poly(A) in buffered solutions of different ionic strength⁵ does not, however, seem to be in accord with the requirements of their mechanism.

Orientation in an electric field is due to the torque exerted by the field on the induced and/or permanent dipole moments of the molecules in the field. Very large moments can be induced in macromolecules through